Available online at www.sciencedirect.com
SCIENCE DIRECT®
Journal of Crystal Growth 287 (2006) 34–38
JOURNAL OF CRYSTAL GROWTH
www.elsevier.com/locate/jcrysgro

Well-ordered ZnO nanowire arrays on GaN substrate fabricated via nanosphere lithography

Hong Jin Fan[a,*], Bodo Fuhrmann[b], Roland Scholz[a], Frank Syrowatka[b], Armin Dadgar[c], Alois Krost[c], Margit Zacharias[a]

[a]*Max Planck Institute of Microstructure Physics, Weinberg 2, 06120 Halle, Germany*
[b]*The Interdisciplinary Center of Materials Science, Hoher Weg 8, Martin-Luther University Halle, Germany*
[c]*Institute of Experimental Physics, Otto-von-Guericke University, 39016 Magdeburg, Germany*

Available online 28 November 2005

Abstract

Nanopatterned ZnO nanowire arrays are fabricated in large scale on epitaxial GaN substrates through a template-controlled process. This process involves nanosphere self-assembly and mask transfer, deposition of Au nanodots, and vapor–liquid–solid (VLS) growth of ZnO nanowires. Self-assembled polystyrene nanospheres are transferred from hydrophilic glass substrate onto hydrophobic GaN layers using an elegantly simple mask transfer technique. Gold is thermally evaporated through the nanosphere mask to form ordered arrays of Au nanodots. Subsequently, ZnO nanowires are grown via VLS epitaxy mechanism catalyzed by the Au nanodots. The diameters and lengths of the nanowires are strongly correlated with the Au dot sizes and growth time, respectively. Cross-sectional transmission electron microscopy studies confirm the VLS epitaxy mechanism and the single crystallinity of the nanowires.

PACS: 61.82.Rx; 81.05.−t; 81.05.Dz; 81.10.−h

Keywords: A1. Nanosphere lithography; A1. Nanostructures; A3. Vapor-phase epitaxy; B1. nanomaterials; B1. Zinc compounds; B2. Semiconducting II–IV materials

1. Introduction

Synthesis of ZnO nanowires with precise control of their alignment, distribution and aspect ratio is highly desirable for their potential applications in sensor arrays, high-efficiency photonic devices, near-UV lasers, and for assembling complex three-dimensional nanoscale systems ([1], and refs therein). A straightforward approach for this purpose is to create metal nanoparticles, which are used as catalyst templates for the subsequent guided vapor–liquid–solid (VLS) growth of nanowires [2]. In the past few years, a number of approaches have been used to obtain nanoscale-patterned metal catalysts for the fabrication of ZnO nanowires arrays. They include electron beam lithography (EBL) [3], soft-photolithography [4], and mask lithography by porous alumina [5], self-assembled micro- or nanospheres [6–8]. EBL is known as a relatively complicated and costly method, thus unsuitable for large-scale fabrication. In contrast, imprint and nanosphere lithography (NSL) tend to be more promising as they are less costly techniques with a much higher throughput. Recently, several groups [6–8] reported the large-scale fabrication of ZnO nanowires templated by NSL. However, the ZnO nanowires in these reports are either not patterned in nanoscale because of the interconnection of the printed Au [6], or not truly vertically aligned [7,8] due to unoptimized growth conditions and/or imperfect lattice matching between the sapphire substrates and ZnO nanowires. These drawbacks might hinder the consideration of such nanowire arrays from device applications.

GaN and ZnO have a similar fundamental bandgap energy (~3.4 eV), the same wurtzite crystal symmetry, and a low misfit of the lattice constant (1.9%). This, as well as the availability of high-quality p-doped GaN films, makes GaN a good candidate for both epitaxial growth [9,10] and

*Corresponding author. Tel.: +49 345 5582760; fax: +49 345 5511223.
E-mail address: hjfan@mpi-halle.de (H.J. Fan).

0022-0248/$ - see front matter © 2005 Elsevier B.V. All rights reserved.
doi:10.1016/j.jcrysgro.2005.10.038

device applications of ZnO nanowires. Recently, we reported a new template method for fabrication of perfect arranged arrays of ZnO nanowires or pillars on GaN epilayers, in which Au nanotube membranes were used as a lithography mask to produce ordered arrays of Au nanodots [10]. In this contribution, we apply the same growth method using a modified NSL technique. The obtained ZnO nanowires have a uniform vertical alignment to the substrate, and nanoscale pattern (i.e., nearly a single wire at each catalytic Au dot site) as defined by the mask.

2. Experiments

The whole fabrication process is schematically illustrated in Fig. 1. First, aqueous solution of 488 nm polystyrene (PS) nanospheres (Nanoparticles GmBH, Germany) was diluted in methanol and spin-coated onto a glass substrate. The glass substrates were cleaned in $NH_4OH/H_2O_2/H_2O$ (1:1:5) at 80 °C for 30 min and stored in water until usage. The PS spheres self-assemble into a monolayer (or bilayer depending on dilution degree and spin speed) structure [7,8,11] (Fig. 1(a)). Afterwards, a ~50 nm thick Au film was deposited on the nanospheres (Fig. 1(b)), forming a continuous coating of Au on the upper part of the hemispheres [12]. The glass substrate coated with the nanospheres was immersed into DI water to separate the sphere layers from the substrate. As a result, the released free-standing membranes (Au-coated membranes of nanospheres) remained floating on the water surface (Fig. 1(c)). The membranes were then transferred onto the surface of GaN/Si by immersing the latter into the solution and lifting up the substrate together with the membrane. Thermal evaporation of gold (Fig. 1(d)) was conducted in a vacuum (5×10^{-4} Pa) chamber through the membrane mask. A nominal thickness of 2–3 nm was used in our experiments. Subsequently, the masks were removed by dissolution in CH_2Cl_2 in an ultrasonic bath for 2 min, exposing the arrays of gold nanodots on the substrate surface (Fig. 1(e)).

Synthesis of ZnO nanowires (Fig. 1(f)) was conducted via vapor transport and deposition in a double-tube system, as described earlier [10]. The temperatures for the source and substrate were 850 and 650 °C, respectively. The morphology was examined using a XL30 ESEM-FEG scanning electron microscopy (SEM). For the transmission electron microscopy (TEM) analysis, cross-sectional TEM samples were prepared through a standard procedure.

3. Results and discussion

NSL has been a widely used technique for structuring substrates with a hexagonal array of various nanomaterials, including ferroelectric [13], magnetic [14,15], and metal dots for growth of carbon nanotubes [16,17] and semiconductor nanowires [6–8], etc. However, a direct deposition of PS nanospheres on GaN was found to be difficult due to the hydrophobicity of GaN. To address this problem, we applied the known "mask transfer" [12] technique as illustrated in Fig. 1, i.e., the nanospheres self-assembled on hydrophilic substrate (glass in this case) were first connected by a thin metal coating, and then transferred to the GaN surface. The mask transfer stabilizes the self-assembled spheres and thus reinforces the feasibility of large-scale Au nanodot arrays on GaN. Fig. 2 shows a part of the deposited Au nanodot array using a monolayer of PS spheres as lithography mask. The nanodots are well separated from each other and have an average diameter of 30 nm and height of 3 nm. It is worth mentioning that the well separation and small size is another advantage of the mask transfer technique. In previously reported NSL, the deposited Au clusters are either interconnected [6], or in an overall size of 100 nm

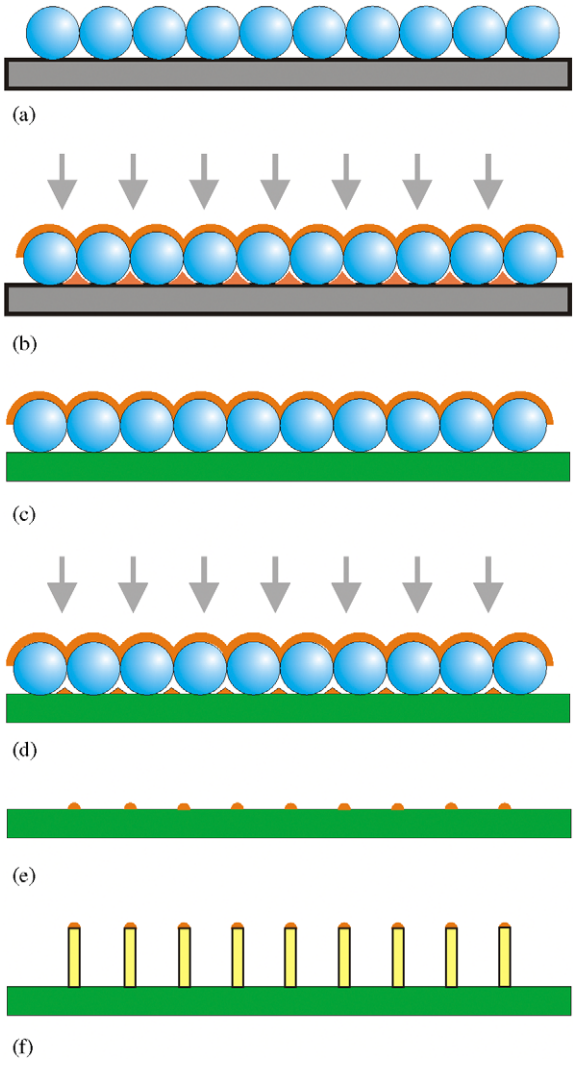

Fig. 1. Schematics of the fabrication process: (a) self-assembly of PS nanospheres spin-coated on a glass substrate, (b) a ~50 nm thick gold film is sputtered onto the PS spheres in order to stabilize the self-assembled structure for the subsequent transfer process, (c) the membrane of Au-stabilized PS spheres is transferred onto the GaN substrate (see text for details), (d) thermal evaporation of gold using the membrane as shadow mask, (e) gold nanodot arrays after removal of the membrane mask and (f) vapor transport and deposition growth of ZnO nanowires via the vapor–liquid–solid epitaxy mechanism.

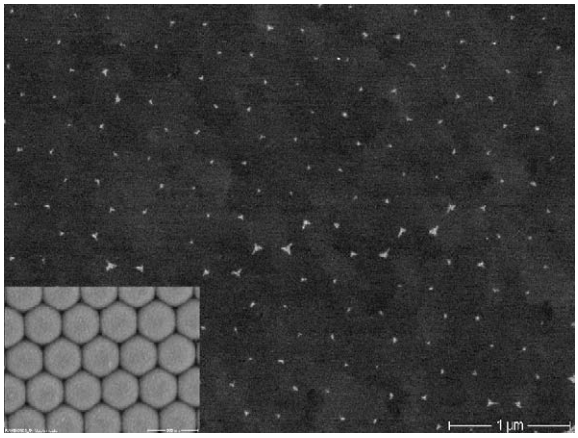

Fig. 2. Au nanodot arrays corresponding to Fig. 1(e). Inset shows the mask on GaN: monolayer of Au coated hexagonally packed PS nanospheres.

[7,8] which is much larger than the desired ZnO nanowire diameters. In our method, the metallic coating of the PS spheres narrows the holes between the spheres, and subsequently decreases the Au dot size. This is highly desirable for subsequent growth of single nanowires on individual Au dots.

Using the Au nanodots as catalyst, ZnO nanowires were grown through the VLSE mechanism on lattice-matched GaN substrate in a double-tube system [10]. It should be stressed that a relative low growth temperature (~650 °C) is crucial to prevent the thermal-induced diffusion of liquid Au, thus preserving the initial periodic pattern during the growth of nanowires. In fact, the use of a small-volume reaction tube and the low substrate temperature are the key to successful fabrication of single wires at individual Au sites. Fig. 3 shows the obtained ZnO nanowire arrays. From the top view in Fig. 3(a), it is clear that the nanowires possess a honeycomb lattice, the same as the initial Au nanodots. Some lines are present analogous to linear defects in crystals, partly because of the size imhomogeneity of the PS spheres. The hexagonal ends of the wires indicate that their main axis direction is [0 0 0 1]. The mean diameter of the ordered nanowires is 63 nm (wires growing from Au film or stripes were not counted). Due to the epitaxial growth, the nanowires are completely perpendicular to the GaN surface. In contrast, when sapphire substrates are used, the ZnO nanowires show also inclined or parallel growth [6,7,9]. Possible reasons for the inclined wires are an epitaxial growth from vicinal *a* planes of sapphire, or from faceted ZnO clusters at the nucleation sites. This emphasizes the belief that the GaN(0 0 0 1) layers are ideal substrates for the fabrication of highly ordered ZnO nanostructures [9].

It is known that the NSL technique also allows the self-assembly of PS spheres into a bilayer structure [7,11]. In this case, the deposited Au nanodots have a smaller size and a different lattice compared to the monolayer structure. When they are used as catalyst for the subsequent growth experiment, the resulting ZnO nanowires exhibit a triangular pattern with a constant interwire distance of ≈488 nm, as shown by the top- and inclined-view SEM images in Fig. 4. The mean diameter of the ordered wires is 53 nm, only slightly smaller than that produced using monolayer nanospheres. Again, all the nanowires are vertically aligned to the substrate surface, which is unsurprising since the epitaxial growth is independent of the type of templates. Some points in the array are missing (see Fig. 4(b)) due to defects in the particle arrays, as is typical for NSL.

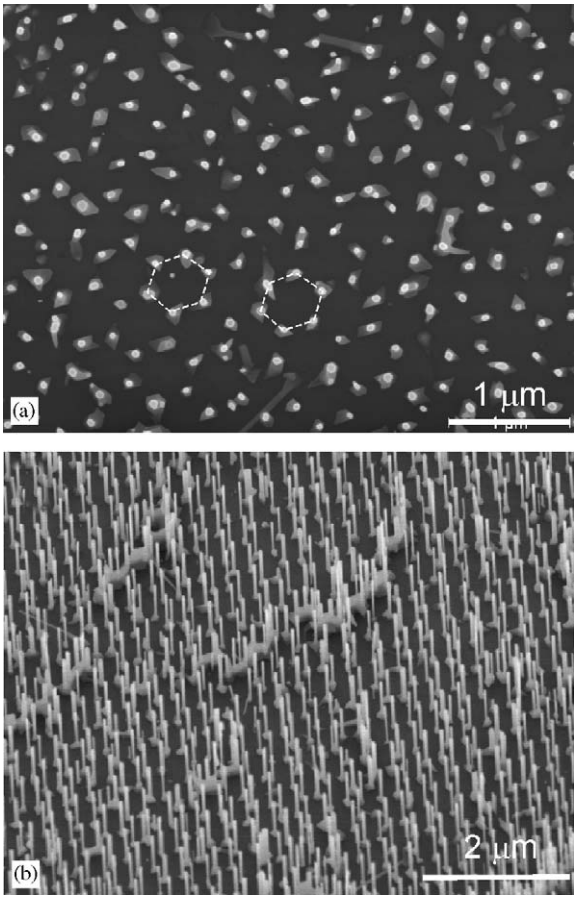

Fig. 3. ZnO nanowire arrays obtained using a monolayer of PS spheres as the template: (a) top view showing that the nanowires have a honeycomb lattice similar to that of Au dots in Fig. 2 and (b) tilted view of the nanowire arrays. The nanowires have a mean diameter of 63 nm.

The above result implies that the diameters of the nanowires depend mainly on the size (including diameter and height) of the catalytic Au dots. The optimum size for growth of a single wire at individual points of the lattice is <50 nm (diameter) and ≈3 nm (height). When Au dots larger than this are used, either there are no nanowires growing at all or multiple nanowires emerge at individual Au sites. The length of the nanowires can be controlled by adjusting the growth time. The optimum time in this case (growth temperature of 640 °C), in order to make the hexagonal pattern distinct after the growth, is 20–30 min. A growth for 30 min led to a nanowire height of 2.5 μm, i.e., a growth rate of approx 83 nm/min. In addition, the growth

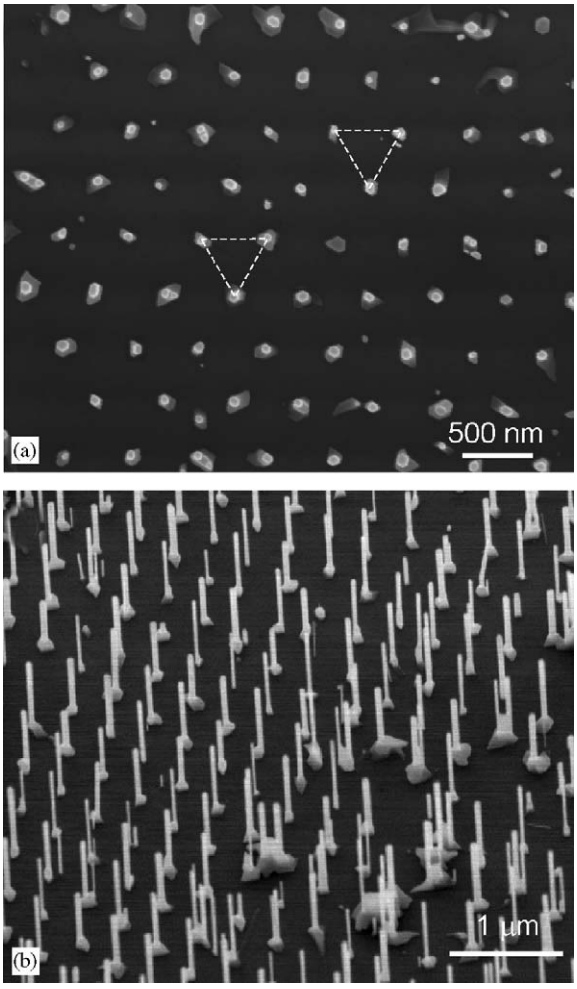

Fig. 4. ZnO nanowire arrays obtained using a bilayer of PS nanospheres as the template: (a) top view showing the triangular lattice of the nanowires and (b) tilted view of the nanowire arrays. The nanowires have a mean diameter of 53 nm.

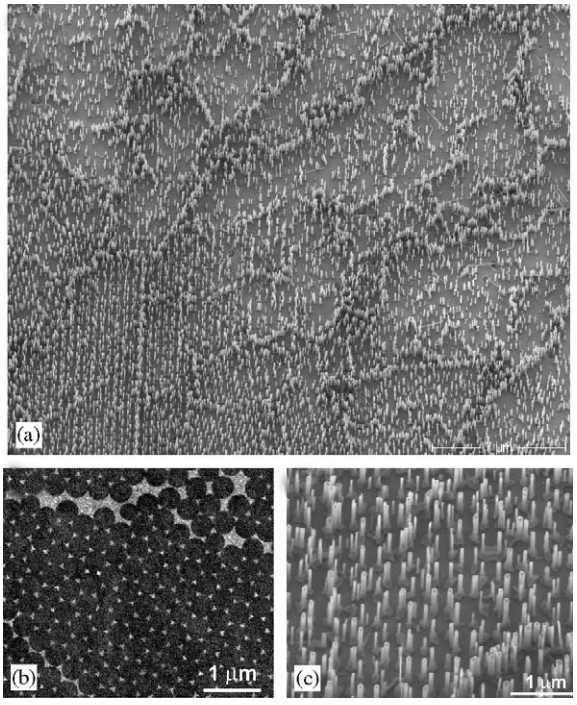

Fig. 5. (a) Typical morphology of ZnO nanowires on a GaN/Si substrate without application of the mask transfer technique. In contrast to results in Figs. 3 and 4, these nanowires have no large-scale periodic arrangement although small quasi-ordered areas are found in some areas (e.g., left-bottom corner). (b) The original template of triangular-shaped Au clusters. (c) Magnified view of the small ordered area showing multiple nanowires at individual Au sites.

rate is also a function of temperature, viz. a higher temperature corresponds to faster growth. This is consistent to findings by other researchers (see for example Ref. [18]). When the temperatures were adjusted to be 870 °C at the source and 670 °C at the substrate, a growth for 30 min resulted in an average nanowire length of 4 μm (i.e., growth rate of approx 130 nm/min).

For comparison, we also conducted the fabrication without application of the mask transfer. In this case, the PS spheres are directly spin-coated on GaN/Si substrates. The conditions for the rest steps, including Au thermal evaporation and nanowire growth, were kept the same. Fig. 5(a) gives a typical view of the sample structure after the ZnO nanowire growth experiment. The nanowires are generally in a disordered distribution, although quasi-ordered arrays are observed in some areas. Reason for this is straightforward, that is, a self-assembly of the PS spheres is not favored on the hydrophobic GaN surface. Fig. 5(b) shows an ordered array of triangular-shaped Au clusters observed in certain places on the substrate surface. Due to the large size of the triangular-shaped clusters (compared to the dots in Fig. 2), growth of 2–3 wires occurred at individual cluster sites, as seen in Fig. 5(c). These corroborate the aforementioned two advantages of the mask transfer technique for large-scale nanopatterned nanowire arrays on the GaN/Si substrates.

The single crystallinity and VLS epitaxy growth mechanism of the ZnO nanowires were verified based on TEM characterizations. In order to prevent the breaking of the nanowires and/or peeling off of the Au tips which can happen during other sample preparation processes (e.g., sonication), we studied the sample from its cross section. Fig. 6(a) displays the low-magnification view of several nanowires on the GaN layer. In addition to the vertical alignment of the nanowires, as consistent to the SEM observations, one can readily see the Au particles present at the tips of the nanowires (exemplified by the dashed circle). This confirms the growth mechanism to be VLS. The selected area electron diffraction patterned (inset in Fig. 6(a)) confirms that the nanowires are wurtzite single crystals with the main axis along the [0 0 0 1] direction. A typical high-resolution TEM image near the nanowire tip is shown in Fig. 6(b), from which the crystal perfection and atomic arrangement of both the nanowire and Au particle can be clearly seen. The corresponding electron diffraction can be indexed to a superimposition of $\{11\bar{2}0\}$ ZnO and $\{\bar{2}20\}$ Au. Furthermore, Fig. 6(b) and (c) also reveal that the Au (1 1 1) planes are parallel to ZnO (0 0 0 2) planes. It

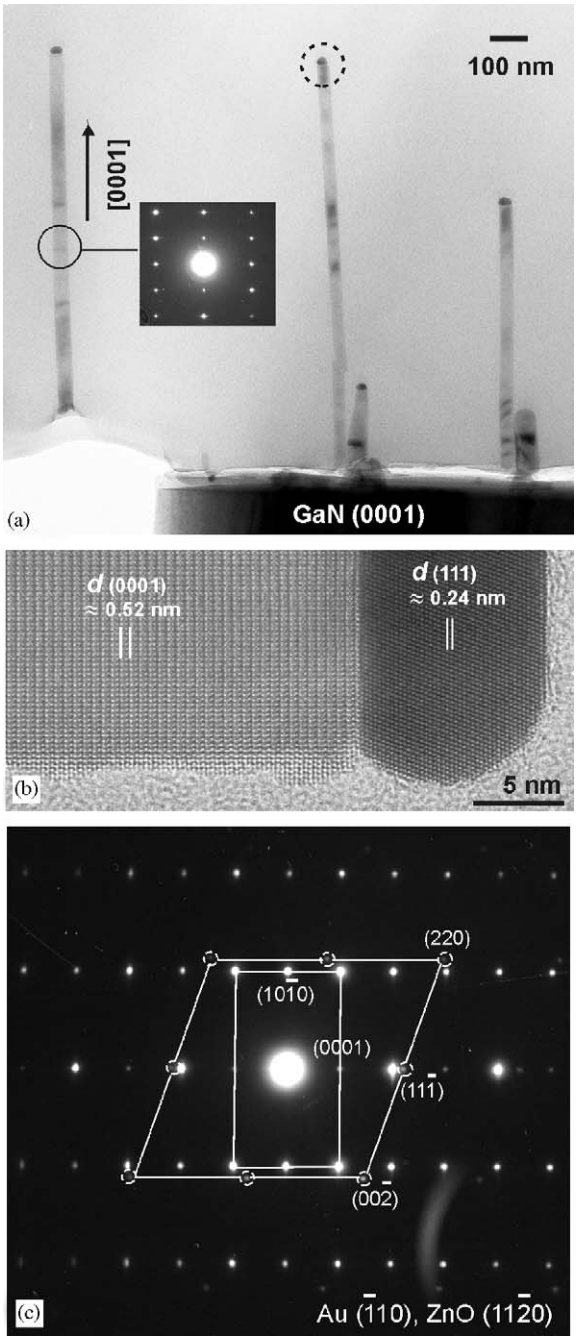

Fig. 6. TEM analysis of the nanowires: (a) a low-magnification cross-sectional view of the nanowires embedded in glue, showing their vertical alignment and the presence of Au tips (indicated by the circle); the inset is the electron diffraction pattern recorded from the circled area, indicating the growth direction along $\langle 0001 \rangle$, (b) high-resolution TEM image near the end of a nanowire, showing the crystalline nature of the nanowire and Au particle and (c) electron diffraction pattern recorded near the end of a nanowire. The diffraction pattern of both ZnO (four-digital index) and Au (three-digital index) are resolved. The transmission direction of the electron beam is along the Au $(\bar{2}20)$ or ZnO $(11\bar{2}0)$ normal.

is worth mentioning that, in certain cases, we also observed Au particles attached on the edge or base of the nanowires (images not shown). This could be a hint that the Au particle can fall down from the wire tip due to some instability, as also observed by Givargizov in his VLS growth of Ge whiskers [19]. More detailed discussions on this will be reported elsewhere.

4. Conclusion

By using nanosphere lithography and mask transfer technique, as well as optimized vapor-phase growth conditions, we fabricated well-ordered and hexagonal-patterned ZnO nanowire arrays in a large scale on epitaxial GaN substrates. Single nanowires at individual catalytic sites are achieved. When the nanospheres are controlled to be mono- or bilayers, the resulting ZnO nanowires have different diameter, geometry and interwire distance. Cross-sectional TEM analysis confirms the vapor–liquid–solid epitaxy mechanism and the single crystallinity of the nanowires. Our fabrication method can be generalized to nanopatterned vertical arrays of other semiconductor nanowires on suitably chosen substrates.

Acknowledgements

We thank M. Hopfe for TEM sample preparation and F. Heyroth for help with SEM.

References

[1] G.-C. Yi, C. Wang, W.I. Park, Semicond. Sci. Technol. (Rev.) 20 (2005) S22.
[2] R.S. Wagner, W.C. Ellis, Trans. Metall. Soc. AIME 233 (1965) 1053.
[3] H.T. Ng, J. Han, T. Yamada, P. Nguyen, Y.P. Chen, M. Meyyappan, Nano Lett. 4 (2004) 1247.
[4] E.C. Greyson, Y. Babayan, T.W. Odom, Adv. Mater. 16 (2004) 1348.
[5] H. Chik, J. Liang, S.G. Cloutier, N. Kouklin, J.M. Xu, Appl. Phys. Lett. 84 (2004) 3376.
[6] X. Wang, C.J. Summers, Z.L. Wang, Nano Lett. 4 (2004) 423.
[7] J. Rybczynski, D. Banerjee, A. Kosiorek, M. Giersig, Z.F. Ren, Nano Lett. 4 (2004) 2037.
[8] D. Banerjee, J. Rybczynski, J.Y. Huang, D.Z. Wang, D. Dempa, Z.F. Ren, Appl. Phys. A 80 (2005) 749.
[9] H.J. Fan, F. Fleischer, W. Lee, K. Nielsch, R. Scholz, M. Zacharias, U. Gösele, A. Dadgar, A. Krost, Superlattices Microstruct. 36 (2004) 95.
[10] H.J. Fan, W. Lee, R. Scholz, K. Nielsch, A. Dadgar, A. Krost, M. Zacharias, Nanotechnology 16 (2005) 913.
[11] J. Rybczynski, U. Ebels, M. Giersig, Colloids Surf. A 219 (2003) 1.
[12] F. Burmeister, C. Schäfele, T. Matthes, M. Böhmisch, J. Boneberg, P. Leiderer, Langmuir 13 (1997) 2983.
[13] W. Ma, C. Harnagea, D. Hesse, U. Gösele, Appl. Phys. Lett. 83 (2003) 3770.
[14] I.J. Martin, J. Nogues, K. Liu, J.L. Vicent, I.K. Schuller, J. Magn. Magn. Mater. (Rev.) 256 (2003) 449.
[15] Y. Wang, J. Rybczynski, D.Z. Wang, Z.F. Ren, Nanotechnology 16 (2005) 819.
[16] K. Kempa, et al., Nano Lett 3 (2003) 13.
[17] Z.P. Huang, et al., Appl. Phys. Lett. 82 (2003) 460.
[18] M.H. Huang, Y. Wu, H. Feick, N. Tran, E. Weber, P. Yang, Adv. Mater. 13 (2001) 113.
[19] E.I. Givargizov, J. Crystal Growth 31 (1975) 20.